

A radical pathway in catecholase activity with nickel(II) complexes of phenol based “end-off” compartmental ligands†

Cite this: *Dalton Trans.*, 2014, **43**, 841

Totan Ghosh,^a Jaydeep Adhikary,^a Prateeti Chakraborty,^a Pradip K. Sukul,^b Mahendra Sekhar Jana,^c Tapan Kumar Mondal,^c Ennio Zangrando*^d and Debasis Das*^a

Seven dinuclear and one dinuclear based dicyanamide bridged polymeric Ni^{II} complexes of phenol based compartmental ligands (HL¹–HL⁴) have been synthesized with the aim to investigate their catecholase-like activity and to evaluate the most probable mechanistic pathway involved in this process. The complexes have been characterized by routine physicochemical studies as well as by X-ray single crystal structure analyses namely [Ni₂(L²)(SCN)₃(H₂O)(CH₃OH)] (**1**), [Ni₂(L⁴)(SCN)₃(CH₃OH)₂] (**2**), [Ni₂(L²)(SCN)₂(AcO)(H₂O)] (**3**), [Ni₂(L⁴)(SCN)(AcO)₂] (**4**), [Ni₂(L²)(N₃)₃(H₂O)₂] (**5**), [Ni₂(L⁴)(N₃)₃(H₂O)₂] (**6**), [Ni₂(L¹)(AcO)₂–N(CN)₂]_n (**7**) and [Ni₂(L³)(AcO)₂–N(CN)₂] (**8**), [SCN = isothiocyanate, AcO = acetate, N₃ = azide, and N(CN)₂ = dicyanamide anion; L^{1–4} = 2,6-bis(R₂-iminomethyl)-4-R₁-phenolato, where R₁ = methyl and *tert*-butyl, R₂ = *N,N*-dimethyl ethylene for L^{1–2} and R₁ = methyl and *tert*-butyl, R₂ = 2-(*N*-ethyl) pyridine for L^{3–4}]. A UV-vis spectrophotometric study using 3,5-di-*tert*-butylcatechol (3,5-DTBC) reveals that all the complexes are highly active in catalyzing the aerobic oxidation of (3,5-DTBC) to 3,5-di-*tert*-butylbenzoquinone (3,5-DTBQ) in methanol medium with the formation of hydrogen peroxide. An EPR study confirms the generation of radicals during the catalysis. Cyclic voltammetric studies of the complexes in the presence and absence of 3,5-DTBC have been performed. Reduction of Ni^{II} to Ni^I and that of the imine bond of the ligand system have been detected at ~–1.0 V and ~–1.5 V, respectively. Coulometric separation of the species at –1.5 V followed by the EPR study at 77 K confirms the species as an organic radical and thus most probably reduced imine species. Spectroelectrochemical analysis at –1.5 V clearly indicates the oxidation of 3,5-DTBC and thus suggests that the radical pathway is supposed to be responsible for the catecholase-like activity exhibited by the nickel complexes. The ligand centred radical generation has further been verified by density functional theory calculation.

Received 31st May 2013,
Accepted 7th October 2013

DOI: 10.1039/c3dt51419f

www.rsc.org/dalton

Introduction

For the last few years our laboratory has been actively engaged to access the mechanistic pathway of catechol oxidase, a less well known member of type-III copper proteins.¹ It is now well established from the reports of several distinguished research groups^{1–11} around the world, including us,^{12,13} that in the case

of Cu^{II} and Mn^{III} model compounds, metal-centered redox participation rather than a radical pathway is most probably responsible for the catecholase activity induced by these species. On the other hand, by using redox innocent Zn^{II} complexes with the “end-off” compartmental ligand,¹⁴ more recently we established that a radical pathway (instead of metal-centered redox contribution) is most probably instrumental in the oxidation of 3,5-di-*tert*-butylcatechol (3,5-DTBC) to 3,5-di-*tert*-butylbenzoquinone (3,5-DTBQ). Moreover, we reported¹⁵ for the first time that a dinuclear Ni^{II} complex with the 2,6-bis(*N*-ethylpiperazine-iminomethyl)-4-methyl-phenol ligand, as a model of the met state of the catechol oxidase, was capable to perform the oxidation of 3,5-DTBC as well as of tetrachlorocatechol, a substrate very hard to oxidize. However, we failed to ascertain the true mechanism operating in that activity. Later on Ghosh *et al.*¹⁶ reported catecholase-like activity with their dinuclear nickel(II) complexes of reduced Schiff-base ligands and commented that a radical pathway was

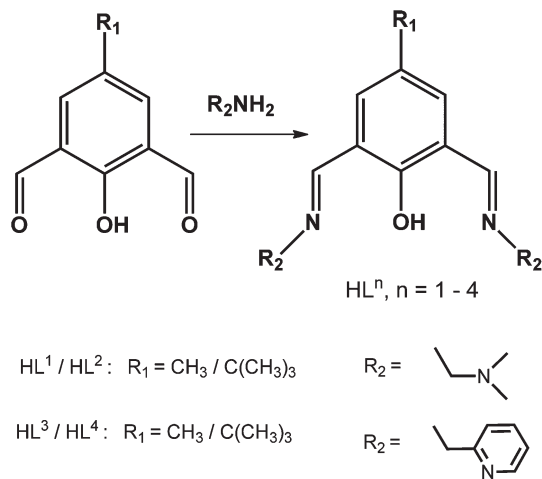
^aDepartment of Chemistry, University of Calcutta, 92, A P C Road, Kolkata-700009, India. E-mail: dasdebasis2001@yahoo.com

^bPolymer Science Unit, Indian Association for the Cultivation of Science, 2A & 2B Raja S. C. Mullick Road, Jadavpur, Kolkata-700032, India

^cDepartment of Chemistry, Jadavpur University, Jadavpur, Kolkata-700 032, India

^dDepartment of Chemical and Pharmaceutical Sciences, University of Trieste, Via L. Giorgieri 1, 34127 Trieste, Italy

† Electronic supplementary information (ESI) available: FT-IR and electronic spectra, cyclic voltammogram, UV-Vis spectroscopic and kinetic data and results of DFT calculations. CCDC 942021–942027 and 942029. For ESI and crystallographic data in CIF or other electronic format see DOI: 10.1039/c3dt51419f



Scheme 1 The four “end-off” compartmental ligands HL^{1–4} used in this study.

operating in that case. Their conclusion was on the basis of the observed isotopic EPR signals at $g \sim 2.00$ after addition of 3,5-DTBC to the complexes. Interestingly, they also observed a very prominent Ni^{III} to Ni^I reduction response in the cyclic voltammetric study. Since no further verification on the origin of the observed EPR signal was reported, it is very difficult to conclude whether the radical pathway or the metal centred redox participation is responsible for catecholase activity of the dinuclear nickel(II) complexes. Further comprehensive investigations are thus necessary to resolve this issue. From that point of view we are reporting herein the syntheses, characterization and catecholase-like activity of eight Ni^{III} complexes, namely [Ni₂(L²)(SCN)₃(H₂O)(CH₃OH)] (1), [Ni₂(L⁴)(SCN)₃(CH₃OH)₂] (2), [Ni₂(L²)(SCN)₂(AcO)(H₂O)] (3), [Ni₂(L⁴)(SCN)(AcO)₂] (4), [Ni₂(L²)(N₃)₃(H₂O)₂] (5), [Ni₂(L⁴)(N₃)₃(H₂O)₂] (6), [Ni₂(L¹)(AcO)₂(N(CN)₂)_n] (7) and [Ni₂(L³)(AcO)₂(N(CN)₂)_n] (8) [where L^{1–4} = phenol based “end-off” compartmental ligand, SCN = isothiocyanate, AcO = acetate, N₃ = azide, and N(CN)₂ = dicyanamide anion]. The Schiff-base ligands L^{1–4}, shown in Scheme 1, were obtained by the condensation of 4-R₁-2,6-diformyl-phenol (R₁ = methyl or *tert*-butyl) with *N,N'*-dimethylethane-1,2-diamine or 2-(2-aminoethyl)pyridine. The detailed structure of eight complexes has been elucidated by X-ray crystallography and 7 shows the formation of a coordination polymer in the solid state. The catecholase activity has been investigated using 3,5-di-*tert*-butylcatechol (3,5-DTBC) as a model substrate. The present study reveals that a radical pathway rather than the metal-centered redox participation is most likely responsible for the catecholase-like activity exhibited by Ni^{III} complexes of “end-off” compartmental Schiff-base ligands.

Results and discussion

Syntheses and characterization

The Schiff-base ligands, HL¹–HL⁴, were synthesized through the classical condensation reaction between 2,6-diformyl-R₁-

phenol (R₁ = methyl or *tert*-butyl) and *N,N*-dimethyl ethylenediamine and 2-(2-aminoethyl)pyridine in methanol medium. The Schiff-base ligands on treatment with nickel(II) salts followed by the addition of NaX [X = SCN, N₃ or N(CN)₂] *in situ* gave us the eight complexes. The complexes were characterized by elemental analysis, IR and UV-vis-NIR spectral study (ESI Fig. S1 to S8 and S56 and S57[†]) and X-ray single crystal structural analyses. All the complexes show bands due to C=N stretch in the range 1630–1685 cm⁻¹ and skeletal vibration in the range 1540–1598 cm⁻¹. IR spectral analyses of 1–3 indicate the presence of thiocyanato ligands in these complexes with different modes of coordination as is evidenced from the splitted band in each case in the range 1996–2090 cm⁻¹, whereas in 4 the thiocyanato ligand should be in a single mode of coordination as it exhibits a single sharp peak at 2096 cm⁻¹. In complexes 5 and 6 the observed splitted band in the range 2035–2285 cm⁻¹ clearly indicates the presence of azido ligands in two different modes of coordination. IR spectral analyses of complexes (7 and 8) indicate the presence of the dicyanamide moiety in them with different modes of coordination as is evidenced from the split band in each case in the range 2160–2300 cm⁻¹. All the complexes show three bands in their electronic spectra (UV-vis-NIR region) suggesting octahedral coordination environment around nickel(II) centres.

Description of crystal structures

All thiocyanate derivatives 1–4 are discrete dinuclear complexes. The X-ray crystallography confirmed that a pair of nickel ions are bridged by the pentadentate ligand L² or L⁴ acting through phenolic oxygen in addition to the imine and the amino nitrogen donors (L²) or py nitrogens (L⁴). In each case the coordination sphere of the metal is a distorted octahedron. The complexes 1 and 2 (shown in Fig. 1 and 2) have a comparable structure comprising of three isothiocyanate anions coordinating *via* nitrogen: one of these acts as bridging species, while two are monodentate and *trans* located with respect to the mean molecular plane. The nickel ions complete their coordination sphere by an aqua and a methanol in 1 and by two methanol molecules in 2, so that in any case an oxygen donor is axially *trans* located to a NCS group. This arrangement favours the formation of weak intramolecular H-bonds between the coordinated methanol (or water) oxygen and the NCS nitrogen of the adjacent axial ligand (O...N distance *ca.* 2.94 Å). The donor set for all metals is N₄O₂. The coordination distances, reported in Table 2, are as expected for this type of complex. It is worth noting that the Ni–NCS bond distances relative to the bridging isothiocyanate are significantly longer (range 2.154(3)–2.254(4) Å) with respect to the monodentate ones (2.055(3) to 2.081(3) Å, Table 2). Moreover the Ni–N(CH₃)₂ bond distances in 1 (of 2.148(3) and 2.159(3) Å) are longer than the Ni–N(py) ones (2.090(3) and 2.103(3) Å) of 2 due to the different hybridization of nitrogen atoms.

With respect to the above described derivatives, one and two isothiocyanates, respectively, are replaced in 3 and 4 by bridging acetate anions (Fig. 3 and 4). In the former the two

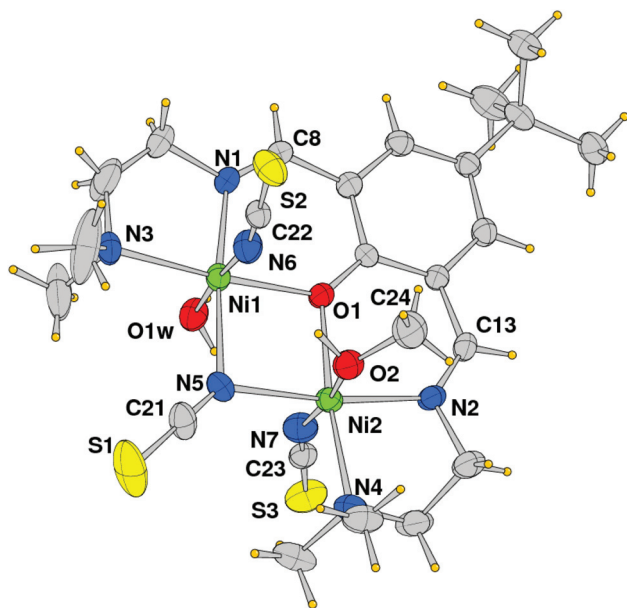


Fig. 1 ORTEP drawing (30% probability ellipsoids) of complex 1 with the atom labelling scheme of the coordination sphere.

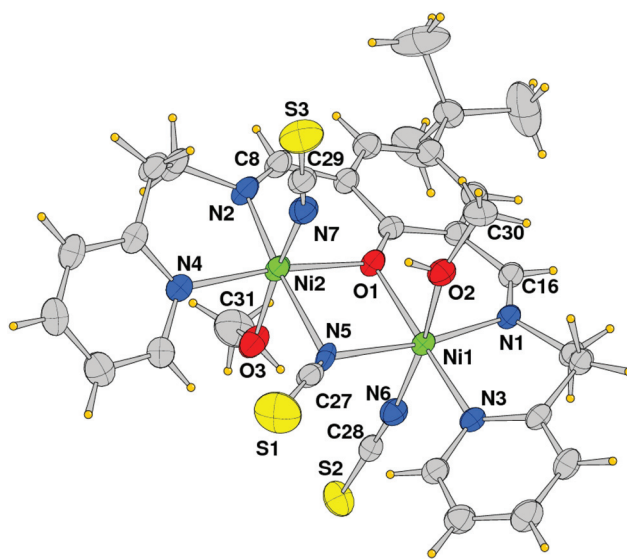


Fig. 2 ORTEP drawing (30% probability ellipsoids) of complex 2.

SCN species behave as bridging and monodentate, while in 4 the unique isothiocyanate occupies an axial position at Ni1. Here the metal chromophores in the two complexes are different, being N_4O_2/N_3O_3 and N_3O_3/N_2O_4 , respectively. It is of interest that in 4, one acetate anion assumes the usual *syn-syn* μ -bridging mode, while the other is monodentate-bridging (μ^3). The latter coordination mode is less frequent²⁶ leading to longer Ni–O bond distances (range 2.150(3)–2.199(3) Å) those involving the *syn-syn* bridging acetate (2.015(3) and 2.087(3) Å, Table 2). The intermetallic Ni1–Ni2 distances are shorter by *ca.* 0.15 Å (compared to 1 and 2), likely affected by triple bridging connections supported by the metals in these cases.

Table 1 Crystallographic data and details of refinement for complexes 1–8

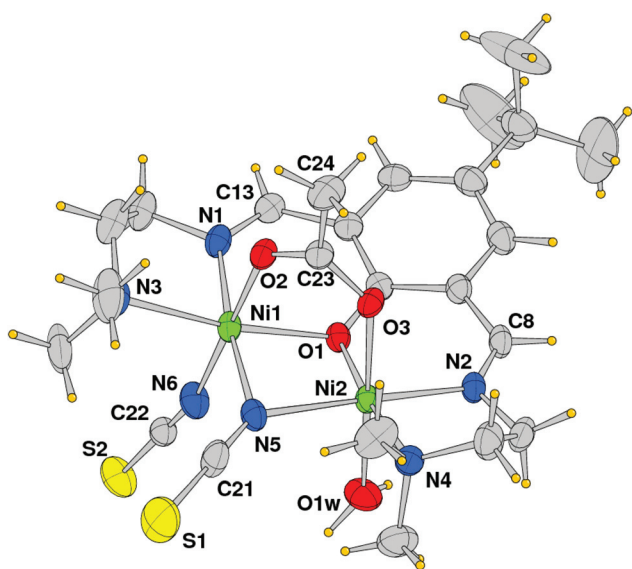
| | 1-CH ₃ OH | 2 | 3-1.5H ₂ O | 4 | 5-CH ₃ OH | 6 | 7 | 8 |
|---|--|--|---|---|--|--|---|---|
| Empirical formula | C ₂₅ H ₃₃ N ₇ Ni ₂ O ₄ S ₃ | C ₃₁ H ₃₇ N ₇ Ni ₂ O ₃ S ₃ | C ₂₄ H ₄₁ N ₆ Ni ₂ O _{5.50} S ₂ | C ₃₁ H ₃₅ N ₅ Ni ₂ O ₅ S | C ₂₀ H ₄₁ N ₁₃ Ni ₂ O ₄ | C ₂₀ H ₃₃ N ₁₃ Ni ₂ O ₃ | C ₂₃ H ₃₃ N ₇ Ni ₂ O ₅ | C ₂₉ H ₂₉ N ₇ Ni ₂ O ₅ |
| Fw | 719.26 | 769.28 | 683.17 | 707.12 | 657.09 | 693.07 | 604.98 | 673.01 |
| Crystal system | Monoclinic | Monoclinic | Monoclinic | Monoclinic | Monoclinic | Monoclinic | Triclinic | Triclinic |
| Space group | <i>P</i> ₂ ₁ | <i>P</i> ₂ ₁ / <i>c</i> | <i>C</i> ₂ / <i>c</i> | <i>P</i> ₂ ₁ / <i>n</i> | <i>P</i> ₂ ₁ / <i>n</i> | <i>C</i> <i>c</i> | <i>P</i> <i>1</i> | <i>P</i> <i>1</i> |
| <i>a</i> (Å) | 9.8340(3) | 14.3491(5) | 24.8159(6) | 12.9741(10) | 11.2211(7) | 13.907(2) | 9.4253(5) | 8.9793(19) |
| <i>b</i> (Å) | 17.6823(6) | 15.1151(5) | 11.8267(3) | 15.3525(12) | 11.8749(7) | 17.381(3) | 12.6299(7) | 12.465(3) |
| <i>c</i> (Å) | 10.1316(4) | 17.3889(6) | 22.4601(6) | 17.3173(14) | 23.0429(15) | 13.590(4) | 13.0653(7) | 14.121(3) |
| α (°) | | | | | | | 100.035(2) | 67.656(2) |
| β (°) | | | | | | | 96.381(2) | 88.238(2) |
| γ (°) | | | | | | | 111.476(2) | 78.297(2) |
| <i>V</i> (Å ³) | 1743.17(11) | 3521.7(2) | 6590.9(3) | 3268.2(4) | 3040.0(3) | 3047.9(11) | 1398.96(13) | 1429.7(5) |
| <i>Z</i> | 2 | 4 | 8 | 4 | 4 | 4 | 2 | 2 |
| <i>D</i> _{calc} (g cm ⁻³) | 1.370 | 1.451 | 1.377 | 1.437 | 1.436 | 1.510 | 1.436 | 1.563 |
| μ (MoK α) (mm ⁻¹) | 1.299 | 1.289 | 1.311 | 1.262 | 1.288 | 1.390 | 1.370 | 1.370 |
| <i>F</i> (000) | 756 | 1600 | 2872 | 1472 | 1384 | 1440 | 632 | 696 |
| θ Range (°) | 2.03–28.49 | 1.52–29.61 | 1.64–27.45 | 1.72–24.17 | 1.79–27.31 | 1.97 to 26.53 | 1.61–25.51 | 1.56–23.85 |
| No. of reflns. collected | 23 821 | 46 159 | 43 023 | 33 174 | 39 244 | 10 892 | 16 496 | 9031 |
| No. of indep. reflns | 7492 | 9108 | 7496 | 5168 | 6805 | 5419 | 5119 | 4353 |
| <i>R</i> (int) | 0.0796 | 0.0265 | 0.0710 | 0.0609 | 0.0738 | 0.0312 | 0.0349 | 0.0270 |
| No. of reflns <i>I</i> > 2 σ (<i>I</i>) | 5291 | 6671 | 4587 | 3991 | 5012 | 5116 | 4064 | 3523 |
| Refined params | 407 | 421 | 376 | 395 | 394 | 409 | 335 | 388 |
| Goodness-of-fit (<i>F</i> ²) | 0.902 | 1.026 | 1.081 | 1.081 | 1.018 | 1.018 | 1.048 | 1.079 |
| <i>R</i> ₁ , <i>wR</i> ₂ (<i>I</i> > 2 σ (<i>I</i>)) ^a | 0.0372, 0.0710 | 0.0564, 0.1614 | 0.0588, 0.1519 | 0.0502, 0.1311 | 0.0412, 0.1034 | 0.0295, 0.0682 | 0.0451, 0.1205 | 0.0393, 0.0971 |
| Residuals (e Å ⁻³) | 0.245, –0.248 | 1.917, –1.018 | 1.134, –0.723 | 0.647, –0.378 | 1.528, –0.598 | 0.469, –0.272 | .489, –0.387 | 0.439, –0.423 |

$$^a R_1 = \sum ||F_o| - |F_c|| / \sum |F_o|, wR_2 = [\sum w(F_o^2 - F_c^2)^2 / \sum w F_o^2]^{1/2}$$

Table 2 Coordination bond distances (Å) and geometrical parameters for compounds 1–4

| | 1·CH ₃ OH | 2 | 3·1.5H ₂ O | 4 |
|-------------------------------|----------------------|-----------|-----------------------|-----------|
| Ni(1)–N(1) | 1.986(3) | 2.007(3) | 1.989(4) | 2.000(4) |
| Ni(1)–N(3) | 2.159(3) | 2.103(3) | 2.180(4) | 2.078(4) |
| Ni(1)–N(5) | 2.154(3) | 2.212(3) | 2.147(4) | 2.059(5) |
| Ni(1)–N(6) | 2.081(3) | 2.055(3) | 2.048(4) | — |
| Ni(1)–O(1) | 2.035(2) | 2.060(2) | 2.043(3) | 2.025(3) |
| Ni(1)–O(2) | — | 2.224(3) | 2.045(3) | 2.150(3) |
| Ni(1)–O(4) | — | — | — | 2.087(3) |
| Ni(1)–O(1w) | 2.120(3) | — | — | — |
| Ni(2)–N(2) | 1.988(3) | 2.005(3) | 1.979(3) | 1.997(3) |
| Ni(2)–N(4) | 2.148(3) | 2.090(3) | 2.155(4) | 2.072(4) |
| Ni(2)–N(5) | 2.168(3) | 2.254(4) | 2.088(4) | — |
| Ni(2)–N(7) | 2.072(3) | 2.075(4) | — | — |
| Ni(2)–O(1) | 2.032(2) | 2.063(2) | 2.028(3) | 2.018(3) |
| Ni(2)–O(2) | 2.151(2) | — | — | 2.120(3) |
| Ni(2)–O(3) | — | 2.164(3) | 2.068(3) | 2.199(3) |
| Ni(2)–O(5) | — | — | — | 2.015(3) |
| Ni(2)–O(1w) | — | — | 2.133(4) | — |
| Ni(1)–Ni(2) | 3.1357(6) | 3.2311(6) | 2.9956(8) | 3.0876(7) |
| <i>d</i> Ni1/Ni2 ^a | 0.037(2) | 0.427(2) | 0.212(3) | 0.301(3) |
| | 0.241(2) | 0.288(3) | 0.334(3) | –0.136(3) |

^a Displacement of metals from the L mean plane.

**Fig. 3** ORTEP drawing (30% probability ellipsoids) of complex 3.

The hexa coordination sphere nickel(II) atoms in complexes 5 and 6 are realised by the bridging 4-*tert*-butylphenolato-O atom, a bridging $\mu^{1,1}$ azide, two monodentate azide anions and two aqua ligands. ORTEP views of the complexes are shown in Fig. 5 and 6. Selected bond lengths relevant to the coordination geometries (Table 3) indicate comparable values to those measured in the complexes described above. Due to the different hybridization of nitrogen donors, the Ni–N(CH₃)₂ bond lengths in 5 (of 2.159(2) and 2.169(2) Å) are longer than the Ni–N(py) ones (2.099(3) and 2.115(2) Å) in 6. The aqua ligands O1w and O2w are involved in intramolecular H-bonds

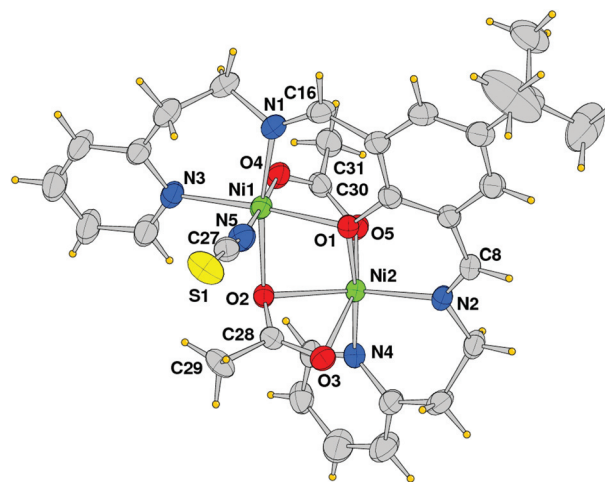
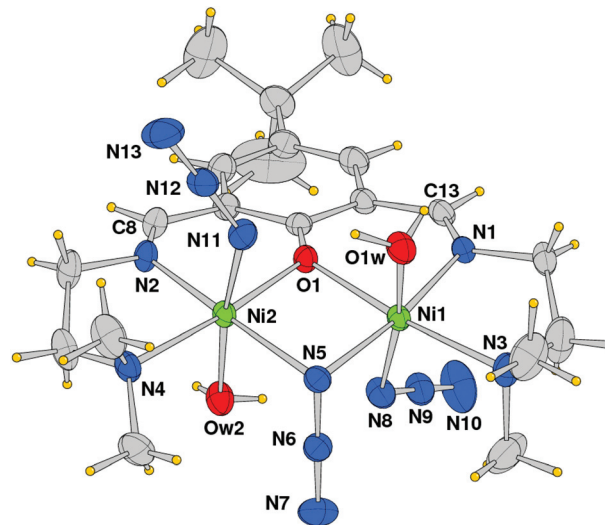
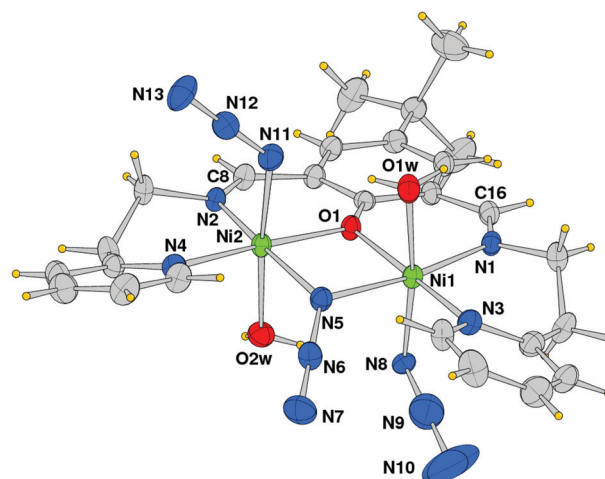
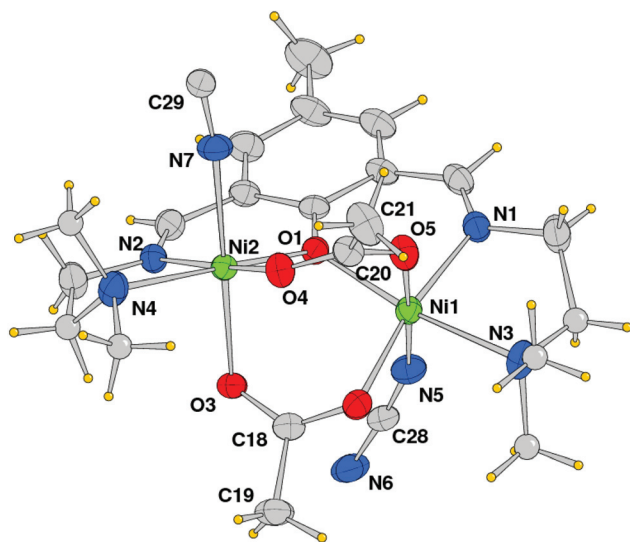
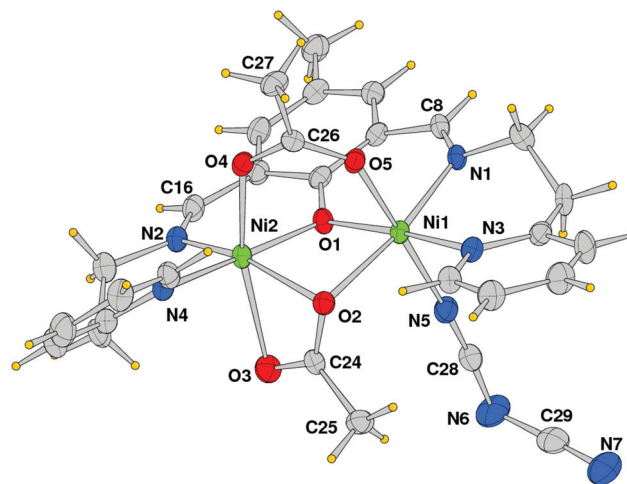
**Fig. 4** ORTEP drawing (30% probability ellipsoids) of complex 4.**Fig. 5** ORTEP drawing (30% probability ellipsoids) of 5. (Of disordered *tert*-butyl groups, only methyl groups at higher occupancy are shown.)**Fig. 6** ORTEP drawing (30% probability ellipsoids) of 6.

Table 3 Coordination bond distances (Å) and geometrical parameters for compounds 5 and 6

| | 5-CH ₃ OH | 6 |
|-------------------------------|----------------------|------------|
| Ni(1)–N(1) | 1.995(2) | 2.000(3) |
| Ni(1)–N(3) | 2.169(2) | 2.115(2) |
| Ni(1)–N(5) | 2.101(2) | 2.110(3) |
| Ni(1)–N(8) | 2.152(2) | 2.179(3) |
| Ni(1)–O(1) | 2.0583(16) | 2.0459(19) |
| Ni(1)–O(1w) | 2.109(2) | 2.146(2) |
| Ni(2)–N(2) | 2.001(2) | 1.997(2) |
| Ni(2)–N(4) | 2.159(2) | 2.099(3) |
| Ni(2)–N(5) | 2.116(2) | 2.127(3) |
| Ni(2)–N(11) | 2.118(2) | 2.111(3) |
| Ni(2)–O(1) | 2.0436(17) | 2.021(2) |
| Ni(2)–O(2w) | 2.171(2) | 2.163(2) |
| Ni(1)–Ni(2) | 3.1089(5) | 3.1612(7) |
| N(9)–N(8)–Ni(1) | 120.35(19) | 119.0(3) |
| N(12)–N(11)–Ni(2) | 125.5(2) | 124.5(2) |
| N(6)–N(5)–Ni(1) | 117.99(18) | 117.2(2) |
| N(6)–N(5)–Ni(2) | 121.15(18) | 120.9(2) |
| <i>d</i> Ni1/Ni2 ^a | 0.570(2) | 0.281(2) |
| | 0.358(2) | 0.087(2) |

^a Displacement of metals from the L mean plane.

**Fig. 7** ORTEP drawing (30% probability ellipsoids) of complex 7. The carbon atoms of the CH₂–N(Me)₂ groups were found disordered.**Fig. 9** ORTEP drawing (30% probability ellipsoids) of complex 8.

with azide nitrogens N11 and N8, respectively, but also with azide of symmetry related complexes.

Derivatives with dicyanamide anions (7–8) have been synthesized for each of the Schiff bases L^{1–4}. In complex 7 each nickel ion exhibits a distorted octahedral geometry comprising the L¹ phenoxido oxygen, the imine and amine nitrogen atoms, and completes its coordination sphere by two oxygen donors from different acetate and a dicyanamide nitrogen atom. Both the acetate anions have an oxygen atom axially located at one metal ion, the second at the equatorial position of the other nickel atom (Fig. 7). The Ni–N(amine) bond distances (2.205(4), 2.212(4) Å) are significantly longer than the Ni–N(imine) ones of 2.011(3) and 2.018(4) Å. The μ_{1,5}-bridging N(CN)₂ anion gives rise to a polymeric species running parallel to the crystallographic axis-*a* (Fig. 8), and separates the metals at 8.028 Å.

On the other hand in complex 8 (Fig. 9) the acetate anions coordinate the metals in a different mode: *syn-syn* μ-bridging and monodentate-bridging (μ³), the second pattern as already observed in complex 4. As a matter of fact the N(CN)₂ anions behave as a terminal monocoordinated ligand and the formation of coordination polymers is not observed. It is difficult

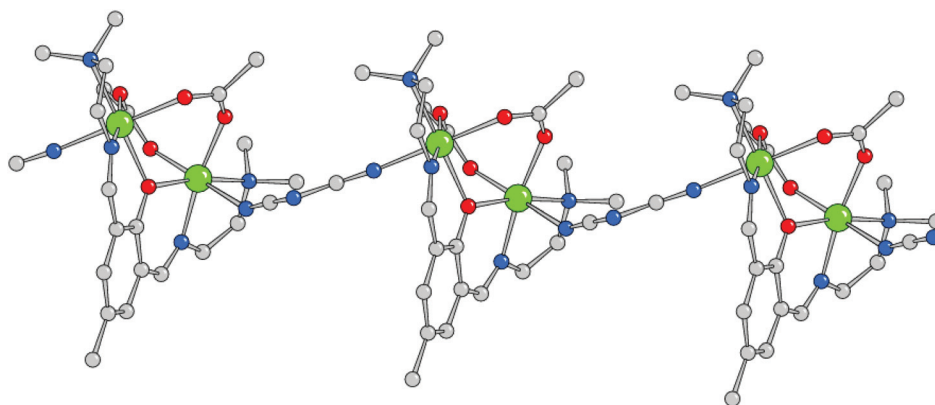
**Fig. 8** The 1D polymeric arrangement of complex 7.

Table 4 Coordination bond distances (Å) and geometrical parameters for complexes **7** and **8**

| | 7 | 8 |
|-------------------------------|-----------|-----------|
| Ni(1)–N(1) | 2.011(3) | 2.012(3) |
| Ni(1)–N(3) | 2.205(4) | 2.083(3) |
| Ni(1)–N(5) | 2.130(4) | 2.092(4) |
| Ni(1)–O(1) | 2.040(3) | 2.040(3) |
| Ni(1)–O(2) | 2.014(3) | 2.150(3) |
| Ni(1)–O(5) | 2.053(3) | 2.069(3) |
| Ni(2)–N(2) | 2.018(3) | 1.998(3) |
| Ni(2)–N(4) | 2.212(4) | 2.066(3) |
| Ni(2)–N(7) | 2.098(4) | — |
| Ni(2)–O(1) | 2.039(3) | 2.024(3) |
| Ni(2)–O(2) | — | 2.117(3) |
| Ni(2)–O(3) | 2.068(3) | 2.246(3) |
| Ni(2)–O(4) | 2.019(3) | 2.015(3) |
| Ni(1)–Ni(2) | 3.3367(7) | 3.0814(8) |
| C(28)–N(5)–Ni(1) | 146.7(4) | 171.6(4) |
| C(29)–N(7)–Ni(2) | 171.9(4) | — |
| <i>d</i> Ni1/Ni2 ^a | 0.650(3) | 0.317(3) |
| | –0.744(3) | –0.202(3) |

^a Displacement of metals from the L mean plane.

to access if the lack of polymer formation is due to packing forces or due to the Schiff base ligand type.

The Ni(1)–Ni(2) distance in **7**, of 3.3375(8) Å, is the longest among the complexes reported here, likely induced by the polymer formation, and confirmed by the metal displacement of 0.65 and –0.74 Å from the phenolato mean plane. In **8** the intermetallic distance is significantly shorter, of 3.0814(8) Å (Table 4).

Catalytic activity

Catecholase activity. All the dinuclear Ni^{II} complexes show significant catalytic oxidation activity towards 3,5-di-*tert*-butylcatechol (3,5-DTBC). This substrate with bulky substituents on the ring has low quinone–catechol reduction potential. This makes it to be easily oxidized to the corresponding *o*-quinone,

3,5-DTBQ, which is highly stable and shows maximum absorption at 401 nm in methanol. Before proceeding into the detailed kinetic study, we started to evaluate the ability of Ni^{II} complexes to oxidize 3,5-DTBC. For this purpose, 1×10^{-4} mol dm⁻³ solutions of complexes **1–8** were treated with 1×10^{-2} mol dm⁻³ (100 equivalents) of 3,5-DTBC under aerobic condition. The course of the reaction was followed by UV-Vis spectroscopy (Fig. S9–S14 in ESI†). The time dependent UV-Vis spectral scan was performed in pure methanol. All the complexes behave similarly, showing a smooth conversion of 3,5-DTBC to 3,5-DTBQ. Fig. 10(a) and (b) show the spectral change for **3** and **5** (as representative dinuclear complexes) upon addition of 100-fold 3,5-DTBC (1×10^{-2} M) observed at an interval of 5 min in CH₃OH. The kinetics of the 3,5-DTBC oxidation was determined by monitoring the increase of the product 3,5-DTBQ. The experimental conditions were same as we reported earlier.¹³ All the complexes showed saturation kinetics and a treatment based on the Michaelis–Menten model seemed to be appropriate. The binding constant (K_M), maximum velocity (V_{max}), and rate constant for dissociation of substrates (*i.e.*, turnover number, k_{cat}) were calculated for all the complexes using the Lineweaver–Burk graph of $1/V$ vs. $1/[S]$ (Fig. S15–S30 in ESI†), using the equation $1/V = \{K_M/V_{max}\} \times \{1/[S]\} + 1/V_{max}$, and the kinetic parameters are presented in Table S1 in ESI†.

The electrochemical analyses reveal that all complexes **1–8** show similar cyclic voltammograms (Fig. S31–S36 in ESI†). Fig. 11(a) and (b) shows the cyclic voltammograms of **3** and **5** as representatives. Complexes **3** and **5** show reduction peaks at –0.95 V and –1.15 V, respectively, which are attributed to the reduction process of Ni^{II} to Ni^I. However, no oxidation peak corresponding to the conversion of Ni^{II} to Ni^{III} is observed in any case. Interestingly, our cyclic voltammetric study of the mixture of complex and 3,5-DTBC (Fig. S37–S44†) exhibits two reductive responses at ~ -1.0 V and at ~ -1.5 V and one oxidative response at $\sim +1.15$ V. The former reduction peak corresponds to the reduction of Ni^{II} to Ni^I and the latter

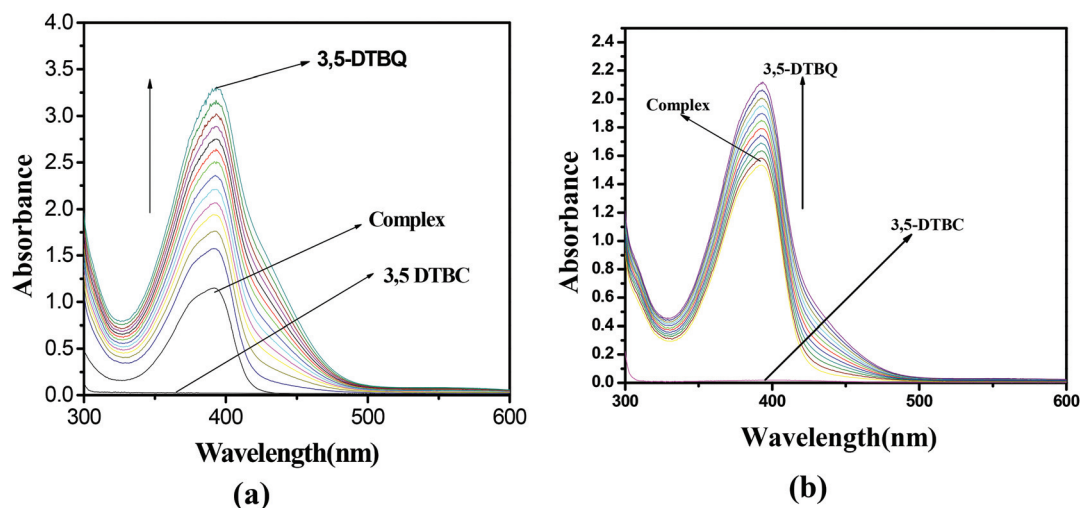


Fig. 10 Changes observed in UV-vis spectra of complexes (a) **3** and (b) **5** (conc. 1×10^{-4} M) upon addition of 100-fold 3,5-DTBC (1×10^{-2} M) in CH₃OH medium.

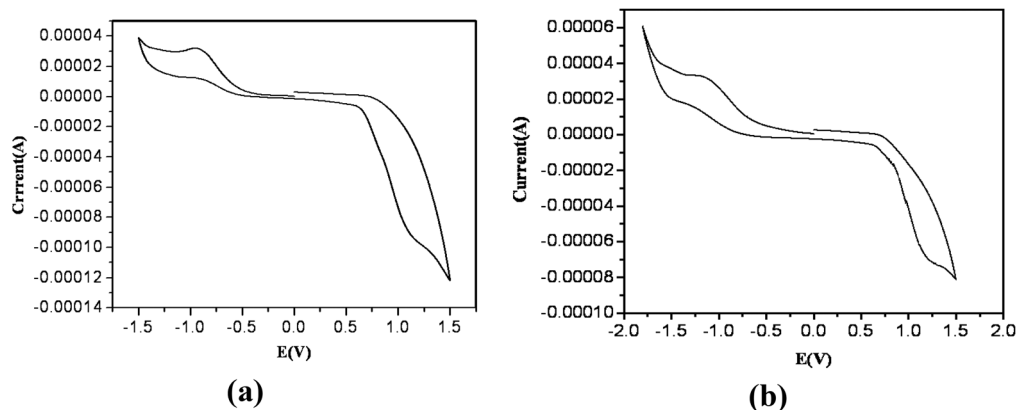


Fig. 11 Cyclic voltammogram of complexes (a) **3** and (b) **5**.

is most likely to be due to the reduction of the C=N bond. The cyclic voltammogram of 3,5-DTBC shows an oxidative response at +1.15 V attributed to the oxidation of 3,5-DTBC to 3,5-DTBQ (Fig. S45[†]) and therefore the observed oxidation peak in the cyclic voltammogram of the mixture of complex and 3,5-DTBC is most likely for that very oxidation.

The conversion of catechol to quinone being a two-electron oxidation process, two different routes may be assumed for nickel complexes to catalyze the aforesaid oxidation: (i) generation of ligand centered free radicals with subsequent oxidation of the substrate or (ii) reduction of Ni^{II} to Ni^I with concomitant oxidation of 3,5-DTBC. In order to verify the possibility of radical participation we have performed the EPR study. The EPR spectra recorded immediately after mixing **3**, **5** and **8** with 3,5-DTBC [Fig. 12(a), (b) and (c), respectively] exhibit broad, nearly isotropic signals at $g \sim 2.00$. Control experiments, under same experimental conditions, indicate that Ni^{II} complexes as well as the mixture of Ni^{II}-salts and 3,5-DTBC are EPR silent. Thus the single EPR line, which is a definite indication of the formation of some ligand centred radical species, is generated only when the Ni^{II} complexes are mixed with 3,5-DTBC and the radical formation is most likely responsible for that oxidation.

The reductive response exhibited by all the complexes at ~ -1.5 V is supposed to be responsible for the oxidation of 3,5-DTBC and in order to get further experimental support for that view we have performed spectroelectrochemical analysis of the complex and 3,5-DTBC mixture (1 : 100) in methanol at -1.5 V. The time dependent spectral scan (Fig. S46[†]) clearly suggests the oxidation of 3,5-DTBC to 3,5-DTBQ. It is now very crucial to determine the electronic structure of the species generated at ~ -1.5 V and for that purpose we have carried out combined coulometric and EPR experiments. The electrogenerated species produced by reductive electrolysis of complex **3** (as representative) and 3,5-DTBC mixture (1 : 100) in methanol in the presence of 0.1 M TEAP exhibits a sharp EPR signal at $g = 1.998$ (Fig. S47[†]) signifying the formation of an organic radical.

On the basis of the above mentioned experimental evidence we may now propose a probable pathway for the catalytic reaction. However, before that we need to know whether dioxygen

reduces to water or H₂O₂ during the oxidation process. The oxidation of I⁻ to I₂ followed by the generation of I₃⁻ as is evident from the UV-vis spectral study of the solution (Fig. S48[†]) obtained after proper work-up of the mixture of catechol, complex **3** and KI (see the Experimental section) clearly hints that dioxygen is reduced to H₂O₂ as is reported by other investigators also.^{2,16,17} It is important to note that whether this hydrogen peroxide is formed from Ni^{II}-O₂²⁻-Ni^{II} or from a superoxide, if any of them produced in the catalytic cycle, are not yet clear to us. At present on the basis of our result we propose a simple mechanistic pathway as depicted in Fig. 13, although the exact catalytic pathway may be very complicated.

DFT study

In order to get a better understanding of the nature of the active species responsible for catecholase activity for the present series of Ni(II) complexes DFT analysis was carried out on complexes **3**, **5** and **8**, as representatives of the present series, and on the corresponding two electron reduced analogues 3²⁻, 5²⁻ and 8²⁻ at the B3LYP level using the Gaussian 03 software package. The most stable structures of **3**, **5** and **8** prove to be open-shell quintet state ($S = 2$) with optimized structural parameters fully consistent with crystallographic data (Fig. S49–S55 in ESI[†] file) and the net spin on Ni(II). The two electron reduced species 3²⁻, 5²⁻ and 8²⁻ display an open-shell ground state with $S = 3$, and the changes in net spin density clearly indicate a ligand centered process for the reductive reaction (Fig. 14–16 respectively). In fact the computational approach shows a significant elongation of the C=N imine bond in the dianionic species (by ~ 0.051 in 3²⁻, 0.044 Å in 5²⁻ and 0.034 Å in 8²⁻ compared to native species (Tables S2–S10[†]), indicating the formation of imine radicals.

Experimental

Physical methods and materials

All materials were obtained from commercial sources and used as received. Solvents were dried according to the standard procedure and distilled prior to use.¹⁸ The 2,6-diformyl-4R-

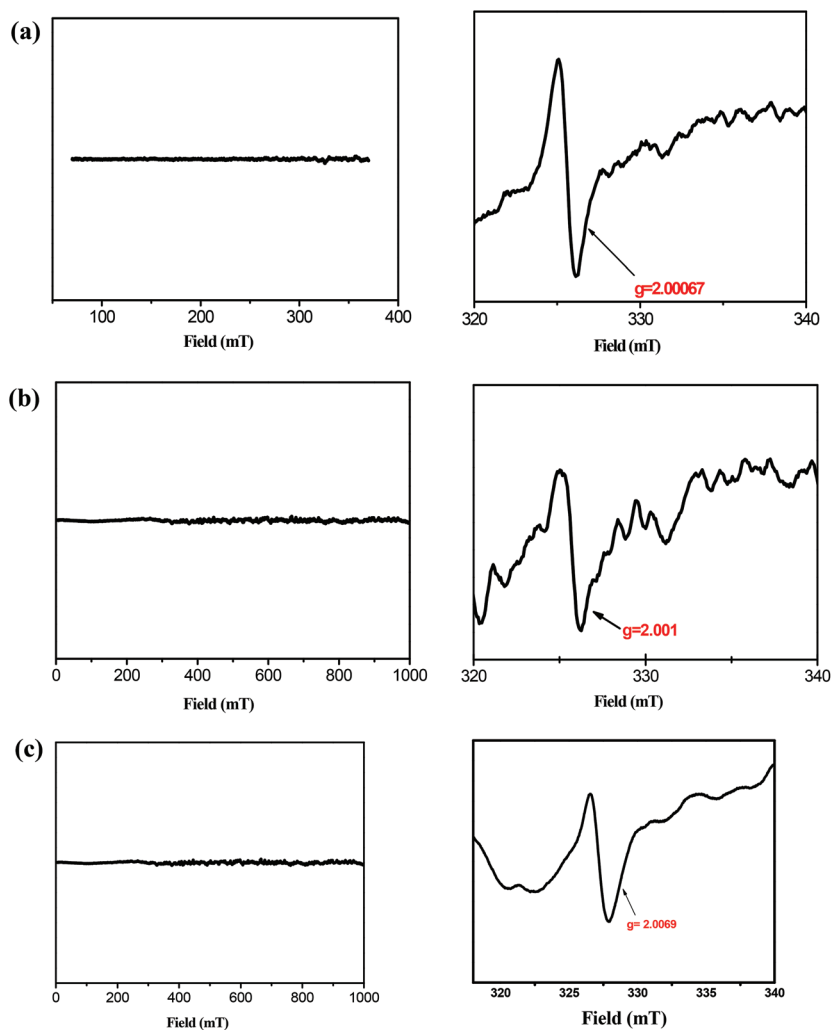


Fig. 12 EPR spectra of the mixture of (a) **3** and **3⁺** 3,5-DTBC; (b) **5** and **5⁺** 3,5-DTBC and (c) **8** and **8⁺** 3,5-DTBC.

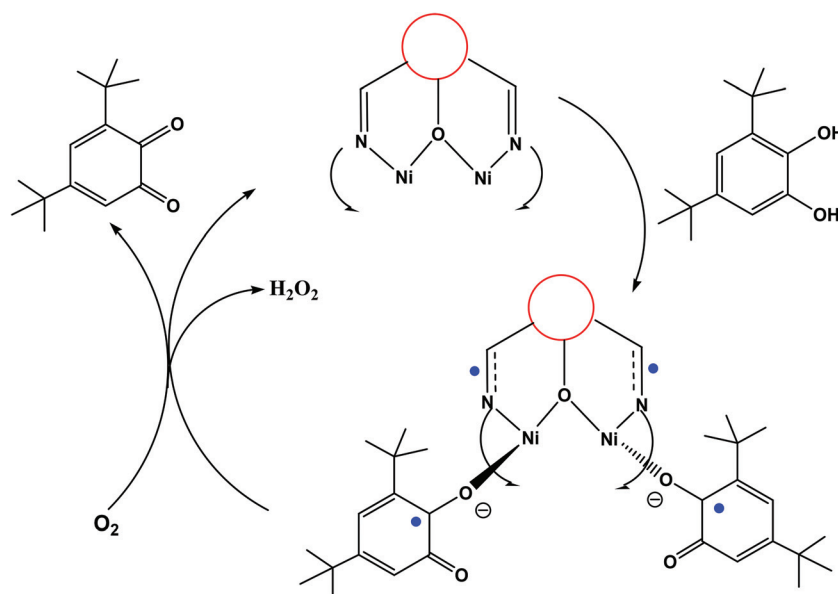


Fig. 13 Proposed mechanism for the catalytic cycle of 3,5-DTBC oxidation by dinuclear Ni^{II} complexes.

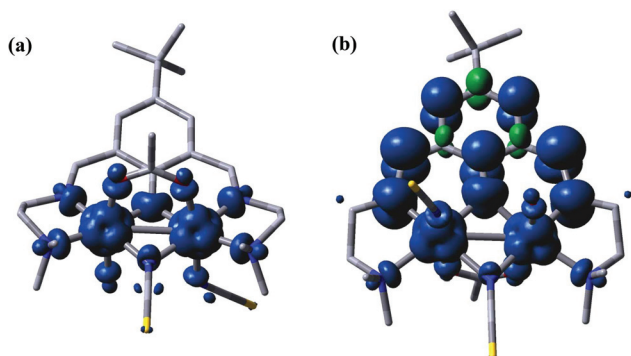


Fig. 14 Spin density plots of (a) **3** ($S = 2$) and of (b) reduced species 3^{2-} ($S = 3$).

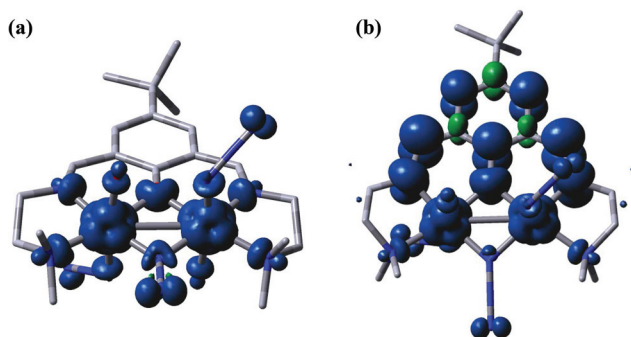


Fig. 15 Spin density plots of (a) **5** ($S = 2$) and of (b) reduced species 5^{2-} ($S = 3$).

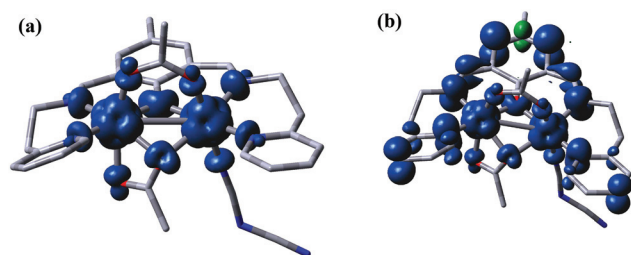


Fig. 16 Spin density plots of (a) **8** ($S = 2$) and of (b) reduced species 8^{2-} ($S = 3$).

phenol (R = methyl and *tert*-butyl) was prepared according to the literature method.¹⁹ Nickel(II) acetate tetrahydrate (Merck), nickel(II) nitrate hexahydrate (Merck), *N,N*-dimethyl ethylenediamine and 2-(2-aminoethyl)pyridine (Aldrich) were purchased from commercial sources and used as received. Elemental analyses (carbon, hydrogen, and nitrogen) were performed using a Perkin-Elmer 240C analyzer. Infrared spectra (4000–400 cm^{-1}) were recorded at 28 °C on a Shimadzu FTIR-8400S using KBr as a medium. Electronic spectra (800–200 nm) were obtained at 27 °C using a Shimadzu UV-3101 PC, where dry methanol was used as a medium as well as a reference. The electron paramagnetic resonance (EPR) experiment was performed at 25 °C and –135 °C in pure

methanol using a Bruker EMX-X band spectrometer and a JEOL JES-FA200 spectrometer. Cyclic voltammograms were recorded in CH_3CN solutions containing 0.1 M TEAP at 25 °C using a three-electrode configuration (Pt working electrode, Pt counter electrode, and Ag/AgCl reference electrode) and a PC controlled PAR model 273A electrochemistry system. The spectroelectrochemical analyses have been done using an electroanalytical instrument BASi Epsilon-EC, and a cell used BASi SEC-C thin-layer quartz glass spectroelectrochemical cell kit (light path length of 1 mm). The supporting electrolyte was –0.2 M tetrabutylammonium hexafluorophosphate in CH_2Cl_2 solution using a three-electrode configuration (Pt working electrode, Pt counter electrode, and Ag/AgCl reference electrode). Spectral data (UV-vis/NIR) were obtained using a Perkin-Elmer Lambda 750 spectrophotometer. Full geometry optimizations of **3**, **7** and **8** and of their reduced species 3^{2-} , 7^{2-} and 8^{2-} were carried out using the density functional theory (DFT) method with the Gaussian 03 package.²⁰ The exchange functional of Becke and the correlation functional of Lee, Yang, and Parr (B3LYP)^{21,22} were employed. To all elements were assigned the 6-31G(d) basis set, except nickel for which the LanL2dz basis set with effective core potential was employed.²³ The vibrational frequency calculations were performed to ensure that the optimized geometries represent the local minima and there are only positive eigenvalues.

Detection of hydrogen peroxide in the catalytic reactions

The formation of H_2O_2 during the catalytic reaction was detected by following the development of the characteristic band for I_3^- spectrophotometrically ($\lambda_{\text{max}} = 353 \text{ nm}$; $\epsilon = 26\,000 \text{ M}^{-1} \text{ cm}^{-1}$), upon reaction with I^- .^{24,25} The oxidation reactions of 3,5-DTBC in the presence of different catalysts were carried out as in the kinetic experiments ($[\text{Complex}] = 2.5 \times 10^{-5} \text{ M}$; $[\text{3,5-DTBC}] = 50 \times 10^{-5} \text{ M}$). After 1 h of reaction an equal volume of water was added and the quinone formed was extracted three times with dichloromethane. The aqueous layer was acidified with H_2SO_4 to pH = 2 to stop further oxidation, and 1 mL of a 10% solution of KI and three drops of 3% solution of ammonium molybdate were added. In the presence of hydrogen peroxide occurs the reaction $\text{H}_2\text{O}_2 + 2\text{I}^- + 2\text{H}^+ \rightarrow 2\text{H}_2\text{O} + \text{I}_2$, and with an excess of iodide ions, the triiodide ion is formed according to the reaction $\text{I}_2(\text{aq.}) + \text{I}^- \rightarrow \text{I}_3^-$. The reaction rate is slow but increases with increasing concentrations of acid, and the addition of an ammonium molybdate solution renders the reaction almost instantaneously. The formation of I_3^- could be monitored spectrophotometrically due to the development of the characteristic I_3^- band $\lambda = 353 \text{ nm}$, $\epsilon = 26\,000 \text{ M}^{-1} \text{ cm}^{-1}$.²⁶

Syntheses of complexes

$[\text{Ni}_2(\text{L}^2)(\text{SCN})_3(\text{H}_2\text{O})(\text{CH}_3\text{OH})]\cdot\text{CH}_3\text{OH}$ (**1**). A methanolic solution (5 mL) of *N,N*-dimethyl ethylenediamine (0.176 g, 2 mmol) was added dropwise to a hot methanolic solution (10 mL) of 2,6-diformyl-4-*tert*-butylphenol (0.206 g, 1 mmol) and the resulting mixture was refluxed for half an hour. Then, a methanolic solution (10 mL) of nickel(II) nitrate hexahydrate

(0.727 g, 2.5 mmol) was added under continuous refluxing condition. After 2 hours an aqueous solution (5 mL) of sodium thiocyanate (0.202 g, 2.5 mmol) was added to the green solution stirring further for 2 h. Single crystals suitable for X-ray analysis were obtained from the filtrate after a few days. Yield: 85%. Anal. Calcd for $C_{24}H_{39}N_7Ni_2O_3S_3 \cdot CH_4O$ ($M = 629.51$ g mol⁻¹): C, 47.69; H, 6.88; N, 15.57. Found: C, 47.73; H, 6.99; N, 15.54. IR: $\nu(SCN) = 2084, 2004$ cm⁻¹, $\nu(C=N) = 1648$ cm⁻¹, $\nu(\text{skeletal vibration}) = 1541$ cm⁻¹.

$[Ni_2(L^4)(SCN)_3(CH_3OH)_2]$ (2). A methanolic solution (5 mL) of 2-(2-aminoethyl)pyridine (0.244 g, 2 mmol) was added dropwise to a hot methanolic (10 mL) solution of 2,6-diformyl-4-*tert*-butylphenol (0.206 g, 1 mmol) and the resulting mixture was refluxed for half an hour. Then, a methanolic solution (10 mL) of nickel(II) nitrate hexahydrate (0.727 g, 2.5 mmol) was added under continuous refluxing condition. After 2 hours an aqueous solution (5 mL) of sodium thiocyanate (0.202 g, 2.5 mmol) was added to the green solution followed by stirring for 2 h. Single crystals suitable for X-ray analysis were obtained from the filtrate after a few days. Yield: 84%. Anal. Calcd for $C_{31}H_{37}N_7Ni_2O_3S_3$ ($M = 769.40$ g mol⁻¹): C, 48.40; H, 4.85; N, 12.75; Found: C, 48.63; H, 4.58; N, 12.54. IR: $\nu(SCN) = 1986, 2059$ cm⁻¹, $\nu(C=N) = 1639$ cm⁻¹, $\nu(\text{skeletal vibration}) = 1542$ cm⁻¹.

$[Ni_2(L^2)(SCN)_2(AcO)(H_2O)] \cdot 1.5H_2O$ (3). The synthesis follows the same procedure adopted for complex 1 by using nickel(II) acetate tetrahydrate (0.620 g, 2.5 mmol), instead of nickel(II) nitrate hexahydrate, in 10 mL of methanol. The resulting green solution was filtered and the filtrate kept in a CaCl₂ desiccator in the dark; square-shaped green crystals were obtained after a few days. Yield 72%. Anal. Calcd for $C_{24}H_{38}N_6Ni_2O_4S_2 \cdot 1.5(H_2O)$ ($M = 683.38$ g mol⁻¹): C, 42.17; H, 6.05; N, 12.30. Found (%): C, 42.27; H, 6.09; N, 11.33. IR: $\nu(SCN) = 2026, 2087$ cm⁻¹, $\nu(C=N) = 1651$ cm⁻¹, $\nu(\text{skeletal vibration}) = 1575$ cm⁻¹.

$[Ni_2(L^4)(SCN)(AcO)_2]$ (4). The complex was synthesized similar to 2 by using a methanolic solution (10 mL) of nickel(II) acetate tetrahydrate (0.620 g, 2.5 mmol) instead of nickel(II) nitrate hexahydrate. The resulting green solution was filtered and the filtrate kept in a CaCl₂ desiccator in the dark; square-shaped green crystals were obtained after a few days. Yield 75%. Anal. Calcd for $C_{31}H_{35}N_5Ni_2O_5S$ ($M = 707.39$ g mol⁻¹): C, 52.66; H, 4.38; N, 9.30; Found (%): C, 52.67; H, 5.01; N, 9.29. IR: $\nu(SCN) = 2096$ cm⁻¹, $\nu(C=N) = 1638$ cm⁻¹, $\nu(\text{skeletal vibration}) = 1574$ cm⁻¹.

$[Ni_2(L^2)(N_3)_3(H_2O)_2] \cdot CH_3OH$ (5). A methanolic solution (5 mL) of *N,N*-dimethyl ethylenediamine (0.176 g, 2 mmol) was added dropwise to a hot methanolic (10 mL) solution of 2,6-diformyl-4-*tert*-butylphenol (0.206 g, 1 mmol) and the resulting mixture was refluxed for half an hour. Then, a methanolic solution (10 mL) of nickel(II) nitrate hexahydrate (0.727 g, 2.5 mmol) was added under continuous refluxing condition. After 2 hours an aqueous solution (5 mL) of sodium azide (0.195 g, 3 mmol) was added to the green solution followed by stirring for 2 h. Single crystals suitable for X-ray analysis were obtained from the filtrate after a few days. Yield: 68%. Anal. Calcd for $C_{19}H_{37}N_{13}Ni_2O_3 \cdot CH_3OH$ ($M = 645.41$ g mol⁻¹):

C, 37.20; H, 6.41; N, 28.21. Found: C, 38.31; H, 6.24; N, 28.23. IR: $\nu(N\equiv N) = 2040, 2077$ cm⁻¹, $\nu(C=N) = 1651$ cm⁻¹, $\nu(\text{skeletal vibration}) = 1575$ cm⁻¹.

$[Ni_2(L^4)(N_3)_3(H_2O)_2]$ (6). The complex was synthesised by a similar procedure as for 5 using a methanolic solution (5 mL) of 2-(2-aminoethyl)pyridine (0.244 g, 2 mmol) instead of *N,N*-dimethyl ethylenediamine for the preparation of the Schiff base. Yield: 70%. Anal. Calcd for $C_{26}H_{33}N_{13}Ni_2O_3$ ($M = 693.39$ g mol⁻¹): C, 45.06; H, 4.80; N, 26.27. Found: C, 45.18; H, 4.75; N, 26.37. IR: $\nu(N\equiv N) = 2036, 2065$ cm⁻¹, $\nu(C=N) = 1639$ cm⁻¹, $\nu(\text{skeletal vibration}) = 1530$ cm⁻¹.

$[Ni_2(L^1)(AcO)_2(N(CN)_2)]_n$ (7). A methanolic solution (5 mL) of *N,N*-dimethyl ethylenediamine (0.176 g, 2 mmol) was added dropwise to a hot methanolic (10 mL) solution of 2,6-diformyl-4-methylphenol (0.164 g, 1 mmol) and the resulting mixture was refluxed for half an hour. Then, a methanolic solution (10 mL) of nickel(II) acetate tetrahydrate (0.620 g, 2.5 mmol) was added under continuous refluxing condition. After 2 hours an aqueous solution (5 mL) of sodium dicyanamide (0.267 g, 3 mmol) was added to the green solution followed by stirring for 2 h. The resulting green solution was filtered and the filtrate was then kept in a CaCl₂ desiccator in the dark, and square-shaped green crystals were obtained after a few days. Yield 79%. Anal. Calcd for $C_{23}H_{33}N_7Ni_2O_5$ ($M = 605.32$ g mol⁻¹): C, 45.62; H, 5.49; N, 16.21. Found (%): C, 46.01; H, 5.09; N, 16.33. IR: $\nu(C\equiv N) = 2178, 2245, 2290$ cm⁻¹, $\nu(C=N) = 1654$ cm⁻¹, $\nu(\text{skeletal vibration}) = 1604$ cm⁻¹.

$[Ni_2(L^3)(AcO)_2(N(CN)_2)]$ (8). A methanolic solution (5 mL) of 2-(2-aminoethyl)pyridine (0.244 g, 2 mmol) was added dropwise to a hot methanolic (10 mL) solution of 4-methyl-2,6-diformylphenol (0.164 g, 1 mmol) and the resulting mixture was refluxed for half an hour. Then, a methanolic solution (10 mL) of nickel(II) acetate tetrahydrate (0.620 g, 2.5 mmol) was added under continuous refluxing condition. After 2 hours an aqueous solution (5 mL) of sodium dicyanamide (0.267 g, 3 mmol) was added to the green solution continuing to stir for 2 h. The resulting green solution was filtered and the filtrate was then kept in a CaCl₂ desiccator in the dark, and needle shaped green crystals were obtained after a few days. Yield 65%. Anal. Calcd for $C_{29}H_{29}N_7Ni_2O_5$ ($M = 673.36$ g mol⁻¹): C, 51.71; H, 4.34; N, 14.57. Found: C, 58.77; H, 4.25; N, 14.62. IR: $\nu(C\equiv N) = 2161, 2264, 2235$ cm⁻¹, $\nu(C=N) = 1651$ cm⁻¹, $\nu(\text{skeletal vibration}) = 1555$ cm⁻¹.

X-ray crystallography

Intensities data for crystal structure analyses of compounds 1–8 were collected on a Bruker Smart Apex diffractometer equipped with CCD. In all cases measurements were conducted at room temperature with MoK α radiation ($\lambda = 0.71073$ Å). Cell refinement, indexing, and scaling of the data sets were done using the programs Bruker Smart Apex and Bruker Saint packages.²⁷ All structures were solved by direct methods and subsequent Fourier analyses²⁸ and refined by the full-matrix least-squares method based on F^2 with all observed reflections.²⁸ The ΔF maps of 1 and 5 revealed the presence of a lattice methanol molecule, that of 3, 1.5 water molecule per

complex unit (H atoms not assigned to the water at half occupancy). Hydrogen atoms were placed at calculated positions and those of lattice water molecules were located on the Fourier map and refined. In compound **1** the carbon atoms of the $-\text{CH}_2-\text{N}(3)(\text{Me})_2$ group was found disordered and refined over two conformations with occupancies of 0.610(13)/0.390(13) and the same disorder was found in **7** both the 5-membered chelate rings (refined occupancies of 0.629(10)/0.371(10) and 0.562(9)/0.438(9)). In **3**, **4** and **5** the *tert*-butyl group was successfully split over two positions (refined occupancies of 0.516(18)/0.484(18), 0.505(10)/0.495(10) and 0.875(9)/0.125(9), respectively). The carbon atoms of disordered groups in **3**, **4** and **7** were isotropically refined. In **2** the N(5)–C(27)–S(1) anion presents N–C and C–S bond distances of 0.914(5) and 1.711(6) Å, possibly contaminated by another ligand, however not evident from ΔF map.

All calculations were performed using the WinGX System, Ver 1.80.05.²⁹ Crystal data and details of refinements are given in Table 1. CCDC 942021–942027 for **1–7** and CCDC 942029 for **8** contain the supplementary crystallographic data for this paper.

Conclusions

In order to unveil the most probable mechanistic pathway followed in catecholase-like activity catalyzed by dinuclear nickel(II) complexes we have synthesized and comprehensively characterized eight nickel(II) complexes of phenol based “end-off” compartmental ligands and investigated their activity towards the aerobic oxidation of 3,5-DTBC in methanol medium. Out of eight complexes seven are dinuclear and one is a coordination polymer in the solid state, but evolves to dinuclear complexes in methanol medium. All complexes are observed to be highly active in catalyzing the aerobic oxidation of 3,5-DTBC to 3,5-DTBQ in methanol. The EPR experiments show generation of ligand centered radicals in the presence of 3,5-DTBC. Although the cyclic voltammetric study of the complexes indicates the reduction of Ni^{II} to Ni^{I} , spectroelectrochemical analysis and the combined coulometric-EPR study suggest that the radical pathway is most likely responsible for the catecholase-like activity exhibited by the nickel complexes investigated in this work. The DFT analyses that confirm a ligand-centered radical in the reduced complexes with significant elongation of imine bond length corroborate well our observed experimental results.

Acknowledgements

The authors wish to thank CSIR, New Delhi [CSIR project No. 01(2464)/11/EMR-II dated 16-05-2011] for financial support. We are thankful to Dr P. Ghosh, Dept. of Chemistry, R. K. Mission Residential College, Narendrapur, Kolkata for spectroelectrochemical analyses. PKS thanks CSIR; TG and JA thank UGC for the fellowship. We also thank the Department

of Science and Technology (DST), New Delhi, for providing single crystal diffractometer facility at the Department of Chemistry, University of Calcutta, through the DST-FIST program.

References

- (a) E. I. Solomon, U. M. Sundaramand and T. E. Machonkin, *Chem. Rev.*, 1996, **96**, 2563–2605; (b) C. Gerdemann, C. Eicken and B. Krebs, *Acc. Chem. Res.*, 2002, **35**, 183–191; (c) I. A. Koval, C. Gamez, P. G. Belle and K. Reedijk, *Chem. Soc. Rev.*, 2006, **35**, 814–840.
- A. Neves, L. M. Rossi, A. J. Bortoluzzi, B. Szpoganicz, C. Wiezbicki and E. Schwingel, *Inorg. Chem.*, 2002, **41**, 1788–1794.
- M. U. Triller, D. Pursche, W. Y. Hsieh, V. L. Pecoraro, A. Rompel and B. Krebs, *Inorg. Chem.*, 2003, **42**, 6274–6283.
- M. Merkel, N. Möller, M. Piacenza, S. Grimme, A. Rompel and B. Krebs, *Chem.–Eur. J.*, 2005, **11**, 1201–1209.
- I. A. Koval, C. Belle, K. Selmecezi, C. Philouze, S. A. Eric, A. M. Schuitema, P. Gamez, J. L. Pierre and J. Reedijk, *J. Biol. Inorg. Chem.*, 2005, **10**, 739750.
- N. N. Murthy, M. Mahroof-Tahir and K. D. Karlin, *Inorg. Chem.*, 2001, **40**, 628–635.
- C. Belle, K. Selmecezi, S. Torelli and J. L. Pierre, *C. R. Chim.*, 2007, **10**, 271–283.
- P. Amudha, M. Kandaswamy, L. Govindasamy and D. Velmurugan, *Inorg. Chem.*, 1998, **37**, 4486–4492.
- J. Mukherjee and R. Mukherjee, *Inorg. Chim. Acta*, 2002, **337**, 429–438.
- C. J. Boxwell, R. Bhalla, L. Cronin, S. S. Turner and P. H. Walton, *Dalton Trans.*, 1998, 2449–2450.
- S. Mandal, J. Mukherjee, F. Lloret and R. Mukherjee, *Inorg. Chem.*, 2012, **51**, 13148–13161.
- K. S. Banu, T. Chattopadhyay, A. Banerjee, S. Bhattacharaya, E. Suresh, M. Nethaji, E. Zangrando and D. Das, *Inorg. Chem.*, 2008, **47**, 7083–7093.
- K. S. Banu, T. Chattopadhyay, A. Banerjee, M. Mukherjee, S. Bhattacharaya, G. K. Patra, E. Zangrando and D. Das, *Dalton Trans.*, 2009, 8755–8764.
- A. Guha, T. Chattopadhyay, N. D. Paul, M. Mukherjee, S. Goswami, T. K. Mondal, E. Zangrando and D. Das, *Inorg. Chem.*, 2012, **51**, 8750–8759.
- T. Chattopadhyay, M. Mukherjee, A. Mondal, P. Maiti, A. Banerjee, K. S. Banu, S. Bhattacharya, B. Roy, D. J. Chattopadhyay, T. K. Mondal, M. Nethaji, E. Zangrando and D. Das, *Inorg. Chem.*, 2010, **49**, 3121–3129.
- A. Biswas, L. K. Das, M. G. Drew, G. Aromí, P. Gamez and A. Ghosh, *Inorg. Chem.*, 2012, **51**, 7993–8001.
- (a) S. Mandal, J. Mukherjee, F. Lloret and R. Mukherjee, *Inorg. Chem.*, 2012, **51**, 13148–13161; (b) S. Fukuzumi, L. Tahsini, Y. M. Lee, K. Ohkubo, W. Nam and K. D. Karlin, *J. Am. Chem. Soc.*, 2012, **134**, 7025–7035.

- 18 D. D. Perrin, W. L. Armarego and D. R. Perrin, *Purification of Laboratory Chemicals*, Pergamon, Oxford, UK, 2nd edn, 1980.
- 19 R. R. Gagne, C. L. Spiro, T. J. Smith, C. A. Hamann, W. R. Thies and A. K. Schiemke, *J. Am. Chem. Soc.*, 1981, **103**, 4073–4081.
- 20 M. J. Frisch, G. W. Trucks, H. B. Schlegel, G. E. Scuseria, M. A. Robb, J. R. Cheeseman, J. A. Montgomery, T. Vreven, K. N. Kudin, J. C. Burant, J. M. Millam, S. S. Iyengar, J. Tomasi, V. Barone, B. Mennucci, M. Cossi, G. Scalmani, N. Rega, G. A. Petersson, H. Nakatsuji, M. Hada, M. Ehara, K. Toyota, R. Fukuda, J. Hasegawa, M. Ishida, T. Nakajima, Y. Honda, O. Kitao, H. Nakai, M. Klene, X. Li, J. E. Knox, H. P. Hratchian, J. B. Cross, V. Bakken, C. Adamo, J. Jaramillo, R. Gomperts, R. E. Stratmann, O. Yazyev, A. J. Austin, R. Cammi, C. Pomelli, J. W. Ochterski, P. Y. Ayala, K. Morokuma, G. A. Voth, P. Salvador, J. J. Dannenberg, V. G. Zakrzewski, S. Dapprich, A. D. Daniels, M. C. Strain, O. Farkas, D. K. Malick, A. D. Rabuck, K. Raghavachari, J. B. Foresman, J. V. Ortiz, Q. Cui, A. G. Baboul, S. Clifford, J. Cioslowski, B. B. Stefanov, G. Liu, A. Liashenko, P. Piskorz, I. Komaromi, R. L. Martin, D. J. Fox, T. Keith, M. A. Al-Laham, C. Y. Peng, A. Nanayakkara, M. Challacombe, P. M. W. Gill, B. Johnson, W. Chen, M. W. Wong, C. Gonzalez and J. A. Pople, *GAUSSIAN 03 (Revision D.01)*, Gaussian, Inc., Wallingford CT, 2004.
- 21 A. D. Becke, *Phys. Rev. A: At., Mol., Opt. Phys.*, 1988, **38**, 3098–3100.
- 22 C. Lee, W. Yang and R. G. Parr, *Phys. Rev. B: Condens. Matter*, 1988, **37**, 785–789.
- 23 P. J. Hay and W. R. Wadt, *J. Chem. Phys.*, 1985, **82**, 270–283.
- 24 (a) E. Monzani, L. Quinti, A. Perotti, L. Casella, M. Gullotti, L. Randaccio, S. Geremia, G. Nardin, P. Faleschini and G. Tabbi, *Inorg. Chem.*, 1998, **37**, 553–562; (b) E. Monzani, G. Battaini, A. Perotti, L. Casella, M. Gullotti, L. Santagostini, G. Nardin, L. Randaccio, S. Geremia, P. Zanello and G. Opromolla, *Inorg. Chem.*, 1999, **38**, 5359–5369.
- 25 J. Ackermann, F. Meyer, E. Kaifer and H. Pritzkow, *Chem.–Eur. J.*, 2002, **8**, 247–258.
- 26 E. Monzani, L. Quinti, A. Perotti, L. Casella, M. Gullotti, L. Randaccio, S. Geremia, G. Nardin, P. Faleschini and G. Tabbi, *Inorg. Chem.*, 1998, **37**, 553–562.
- 27 *SMART, SAINT, Software Reference Manual*, Bruker AXS Inc., Madison, WI, 2000.
- 28 G. M. Sheldrick, *Acta Crystallogr.*, 2008, **64**, 112–122.
- 29 L. J. Farrugia, *J. Appl. Crystallogr.*, 1999, **32**, 837–838.